Kinetics from free-energy landscapes - how to turn phase diagrams into kinetic maps

2000 J. Phys.: Condens. Matter 12 A269

(http://iopscience.iop.org/0953-8984/12/8A/334)

J. Phys.: Condens. Matter **12** (2000) A269–A274. Printed in the UK PII: S0953-8984(00)06927-7

Kinetics from free-energy landscapes—how to turn phase diagrams into kinetic maps

W C K Poon, F Renth and R M L Evans

Department of Physics and Astronomy, The University of Edinburgh, Mayfield Road, Edinburgh EH9 3JZ, UK

Received 3 August 1999

Abstract. We show how the free-energy landscape of a system, normally used only for calculating its *equilibrium* phase diagram, can be used to predict the kinetic pathways that are permitted in the course of phase separation. Applications to one particular soft condensed matter system, a colloid–polymer mixture, are briefly described.

1. Introduction

Gibbs and Boltzmann gave us a recipe for calculating the *equilibrium* phase behaviour of an N-particle system with potential energy $U(\vec{r}_N)$ at temperature T and confined to volume V: minimize the Helmholtz free energy

$$F = -k_B T \ln \int \mathrm{e}^{-U(\vec{r}_N)/k_B T} \, \mathrm{d}\vec{r}_N. \tag{1}$$

The results of this minimization are plotted as phase diagrams for comparison with experiment. To make our discussion concrete, figure 1 shows the temperature–density (T, ρ) projection of the phase diagram of a simple substance such as argon.

The algebraic problem of minimizing (1) can be recast in geometric language in terms of the 'free-energy landscape', a plot of the free-energy density, $f = F/V$, as a function of the density, $\rho = N/V$. All tractable approximations to F give rise to distinct *branches* in the $f(\rho)$ plot for structures of different symmetries. For argon, $f(\rho)$ shows a fluid branch, $f_{\mathrm{F}}(\rho)$, and a solid (crystal) branch, $f_{\mathrm{S}}(\rho)$, for amorphous and ordered arrangements of particles respectively. $f_{\mathrm{S}}(\rho)$ always has a single minimum, while $f_{\mathrm{F}}(\rho)$ can display one or two minima, depending on the temperature.

Figure 2(a) shows the schematic free-energy landscape of argon at a temperature T_0 just below the triple coexistence temperature, T_{tr} (see figure 1). The three minima on this free-energy landscape can, loosely, be associated with the gas, liquid and solid (crystal) phases. Now construct the lowest *common tangent*, and obtain the points of common tangency, ρ_1 and ρ_2. It is easily shown [1] that to minimize F (or, equivalently, f, because V is constant), the system remains in a single, dilute, amorphous phase (gas) at all densities $\rho < \rho_1$, and a single, dense, ordered phase (solid) at all densities $\rho > \rho_2$. At intermediate densities, the lowest F is obtained by the system phase separating into coexisting gas and solid phases at densities ρ_1 and ρ_2 respectively. At T_0 there is no thermodynamically stable liquid phase.

This common-tangent construction gives no information on *processes*—how does a homogeneous dense fluid at temperature T_0 and density (say) ρ_0 (see figure 1) actually phase

0953-8984/00/SA0269+06$30.00

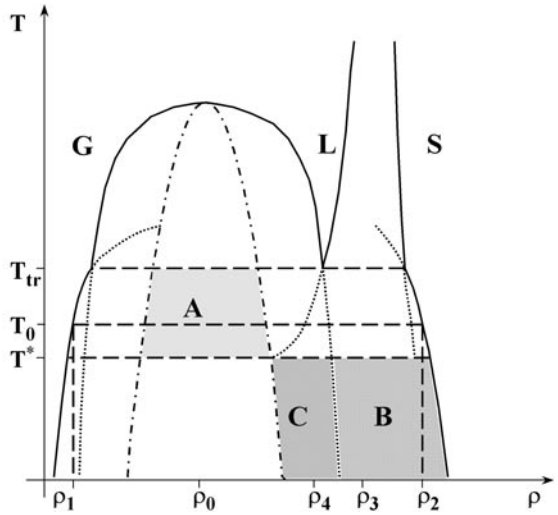

Figure 1. The temperature–density (T, ρ) projection of the phase diagram of a simple substance such as argon. Phase boundaries are shown by continuous lines. Single phases occur in the regions G (gas), L (liquid) and S (solid). Coexistence of two phases occurs between the respective phase boundaries. Triple coexistence occurs at the triple temperature $T_{\rm tr}$. The dotted curves are the metastable continuations of the gas–liquid, gas–solid and liquid–solid phase boundaries. The metastable liquid–solid boundary terminates at the temperature $T^\star$. The dash–dotted curve is the gas–liquid spinodal. The shaded regions A, B and C give rise to kinetic pathways discussed in the text. Note that this is also the phase diagram of a colloid–polymer mixture with large enough polymer-to-colloid size ratio; in this case the vertical axis represents $\tau = k_B T/|U^0_{\rm dep}|$, the inverse dimensionless depletion potential at contact.

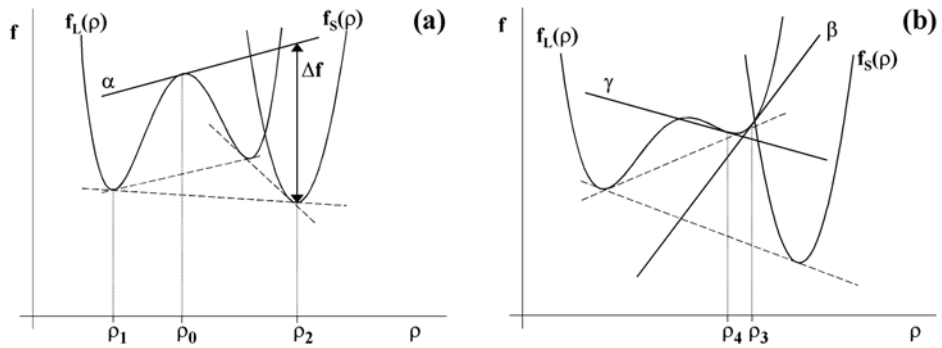

Figure 2. Free-energy landscapes at temperatures (a) $T = T_0$, (b) $T < T^\star$ (see figure 1). See the text for a discussion.

separate into the final equilibrium state of macroscopically coexisting regions of gas and crystal at densities ρ_1 and ρ_2? This *kinetics* question is hard for both theory and experiment. Theoretically, a common way to tackle it is via various phenomenological models [2]. Thus, 'model B' gives the following equation of motion for a conserved 'order parameter' (e.g. the space- and time-dependent density, $\rho(\vec{r}, t)$):

$$\frac{\partial \rho}{\partial t} = \nabla\left[M(\rho)\,\nabla\left(\frac{\partial f(\rho)}{\partial \rho} - \kappa\,\nabla^2\rho\right)\right]. \tag{2}$$

Equation (2) is a highly non-trivial non-linear partial differential equation even for simple forms of $f(\rho)$, and involves phenomenological mobility and curvature coefficients, $M(\rho)$ and κ, which are generally unknown.

In this paper we expound instead a simple but somewhat neglected procedure (due first to Cahn [3]) for turning phase diagrams into 'kinetic maps'—a delineation on the phase diagram of regions of different possible kinetic pathways for phase-separation processes. Once $f(\rho)$ is known, this procedure involves almost no further mathematical effort. On the other hand, the predictions it gives are 'permissive' rather than 'predictive', i.e. they limit possible kinetic pathways without giving any guidance on how to choose between permitted alternatives or predicting any actual rates. Further progress can, however, often be made by making 'educated guesses' [4].

2. The key graphical construction and its implications

Consider again the free-energy landscape in figure 2(a). An $f(\rho)$ with three minima is generic to a number of soft condensed matter systems, e.g. AOT/oil/brine, where the three minima correspond to $L_1/L_\alpha/L_3$ phases [5]. For concreteness, however, we continue for the moment to label the three minima 'gas', 'liquid' and 'solid' (crystal). Instead of the question of equilibrium phase coexistence, let us now ask: how much free energy is available to precipitate an infinitesimal amount of a crystal of density ρ_2 from a homogeneous fluid at density ρ_0? The answer, again easily shown using the same mathematics as leads to the common-tangent construction, is given [3] by the vertical distance between the tangent to the fluid branch; at ρ_0 and the point $f_S(\rho_2)$ on the solid branch; figure 2(a). Below, we discuss the kinetic implications of this 'Cahn construction' using worked examples.

2.1. Worked example (1)

Take a homogeneous fluid at ρ_0 in the free-energy landscape in figure 2(a) (see also figure 1). The tangent α to the fluid branch at this point is above all three minima, i.e. positive free energy is available to precipitate out infinitesimal amounts of gas, liquid or crystal. Here the Cahn construction alone gives a maximally permissive prediction. 'Educated guesses' can take us further. Note that $f_L''(\rho_0) < 0$ (where a prime denotes differentiation with respect to ρ), so the homogeneous fluid is unstable towards local density fluctuations—(T_0, ρ_0) is within the gas–liquid 'spinodal' line [2]. Spinodal decomposition, because it involves no energy barriers, is fast. It is therefore likely (here is the 'educated guess'!) that the homogeneous system will first phase separate into gas and liquid by this route, and then crystals will nucleate out of the denser liquid regions (and, to a lesser extent, the gas regions) subsequently. We call this scenario A.

2.2. Worked example (2)

Turn now to the $f(\rho)$ plot in figure 2(b). The difference from figure 2(a) is that $f_S(\rho)$ is now so much *lower* relative to $f_L(\rho)$ that *no common tangent can be drawn between the solid and liquid minima*. Consider first a homogeneous fluid ('liquid') with density ρ_3. The tangent β to the fluid branch at this point is *below* the gas minimum but *above* the solid minimum. Thus, the system cannot nucleate (at least initially) gas bubbles. Instead, it must first nucleate crystallites. However, since no common tangent can be drawn between the solid and liquid minima, no stable local interface between any crystallite and the surrounding liquid is possible. Common tangents can, however, be drawn between the solid and gas minima, and between

the gas and liquid minima. Thus, the system can only nucleate a crystallite that is coated by a layer of gas which coexists in local equilibrium with both the crystallite and the surrounding liquid. We call this scenario B.

If the density of the initial homogeneous liquid is decreased slightly to ρ_4, figure 2(b), the 'Cahn tangent' (γ) is then above both the gas and solid minima. The system can now nucleate gas bubbles or gas-coated crystals, either sequentially or simultaneously. We call this scenario C.

3. Carving up the phase diagram into kinetic regions

The *equilibrium* phase boundaries plotted in figure 1 are obtained by constructing the *lowest* common tangents on the free-energy landscapes at different temperatures. Various 'metastable phase boundaries', however, can be constructed by drawing higher common tangents, such as the liquid–solid and gas–liquid common tangents constructed in figure 2(a). These give 'metastable continuations' of the various equilibrium phase boundaries, which are shown as dotted curves in figure 1. Also shown (dash–dotted curve) is the gas–liquid spinodal, the locus of inflection points on the liquid branch of the free-energy landscape (i.e. $f_{\mathrm{L}}''(\rho) = 0$). At T^* the low-density branch of the metastable continuation of the liquid–crystal coexistence boundary meets the gas–liquid spinodal and terminates; there is no common tangent between the crystal and liquid minima in the free-energy landscape below this temperature.

These various curves demarcate different *kinetic regions*—the Cahn construction gives distinct permitted kinetic pathways for homogeneous samples belonging to different regions. A moment's thought would now show that the regions labelled A, B and C should give rise to the behaviours with those labels considered in section 2.

4. Colloid–polymer mixtures

We now apply these rules to explain the phase-separation kinetics of one particular soft condensed matter system, a mixture of hard-sphere colloids and non-adsorbing polymer. Experimental details have been given before [6]. Here we emphasize a generic aspect of the problem—time-evolving free-energy landscapes.

The addition of polymers (radius of gyration r_g) to a hard-sphere colloid (radius R) induces an attraction between the particles. Polymer segments are depleted from a layer of thickness $\sim r_g$ around each particle. The overlap of the 'depletion layers' of two nearby particles creates additional free volume for the polymer, lowers the free energy and causes an effective interparticle 'depletion' attraction:

$$U_{\mathrm{dep}}(r) = -\Pi_{\mathrm{P}} V_{\mathrm{ov}}(r) = -(n_{\mathrm{P}}^* k_B T) V_{\mathrm{ov}}(r) \tag{3}$$

where Π_{P} is the osmotic pressure of the polymer and $V_{\mathrm{ov}}(r)$ is the volume of overlap of neighbouring depletion layers. The second equality is for an ideal polymer at number density n_{P}^* *in the free volume*. n_{P}^* is related to the polymer chemical potential μ_{P} (and its de Broglie thermal wavelength Λ_{P}) by [7]

$$n_{\mathrm{P}}^* = \Lambda_{\mathrm{P}}^{-3} \mathrm{e}^{\mu_{\mathrm{P}}/k_B T}. \tag{4}$$

The topology of the phase diagram of a colloid–polymer mixture depends on the size ratio $\xi = r_g/R$. We concentrate on the case of $\xi \gtrsim 1/3$, when the phase diagram shows colloidal gas, liquid and crystal regions [7]. If we use as variables the colloid volume fraction, ϕ, and the inverse dimensionless depletion potential at contact (i.e. $r = 2R$ in (3)), $\tau \equiv k_B T/|U_{\mathrm{dep}}^0|$,

then the phase diagram is similar to that shown in figure 1. In particular, triple coexistence occurs along a *line*—coexisting phases of colloidal gas, liquid and crystal have different ϕ, but identical $\mu_P = \mu_P^{tr}$ (see (3) and (4)). Since τ here takes the role of the temperature T in the argon phase diagram, this variable, or equivalently n_P^* or μ_P, controls the shape of the free-energy landscape in a colloid–polymer mixture.

Experimentally, the directly controllable variable is not μ_P (or, equivalently, n_P^*) but the polymer number density in the *total* volume, n_P. On the (ϕ, n_P) phase diagram, triple coexistence shows up as a triangular region. A homogeneous sample within the triangle separates into gas, liquid and solid phases with compositions given by its corners. In a sample that has macroscopically separated into these phases, $\mu_P = \mu_P^{tr}$, and the three minima on its free-energy landscape lie on a single common tangent. When such a sample is homogenized, however, the polymer chemical potential rises, $\mu_P > \mu_P^{tr}$, and the liquid minimum becomes metastable. The free-energy landscapes shown in figure 2 are therefore appropriate for homogeneous colloid–polymer mixtures with compositions within the triple triangle. The different kinetic regions on the (ϕ, τ) phase diagram (cf. figure 1) can be mapped onto the (ϕ, n_P) phase diagram, dividing, in particular, the three-phase triangle into regions where different kinetic pathways are expected. These kinetic regimes have been observed [6]. In figure 3 we show micrographs demonstrating the scenario A discussed in section 2.1.

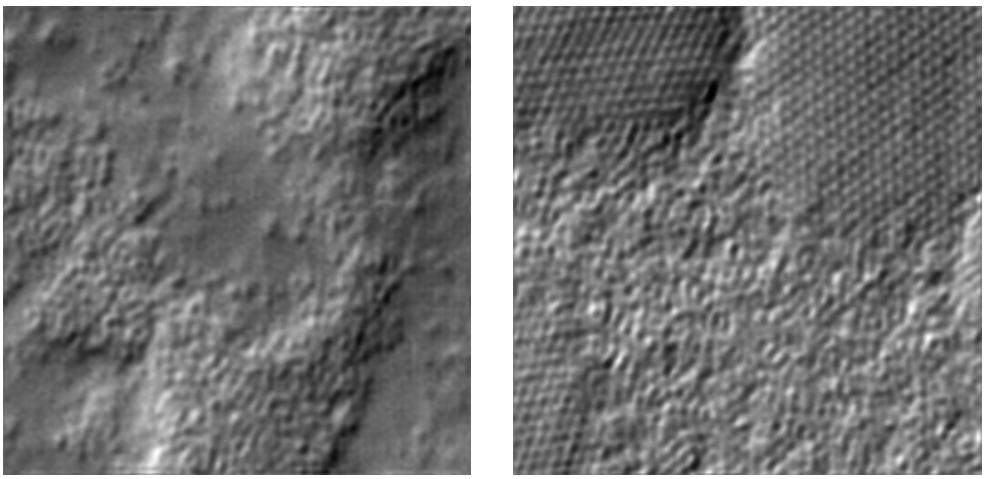

Figure 3. The left-hand micrograph shows the early stages of phase separation in a colloid–polymer mixture showing the behaviour labelled A in the text, with a bicontinuous structure of colloidal liquid and gas indicating spinodal decomposition taking place. As the colloidal particles are denser than the surrounding liquid, the liquid phase gathers at the bottom of the sample cell, with the gas phase on top. Later, crystallization starts within the liquid phase (right-hand micrograph).

The above discussion is based on the premise that the shape of $f(\rho)$ (and therefore the kinetic map) of a colloid–polymer mixture is controlled by the polymer chemical potential. This is equivalent to assuming that of the two concentrations, ϕ and n_P, the latter is the fast variable. This is a reasonable assumption for the mixtures that we studied, where $\xi \lesssim 0.4$. Thus, while μ_P continuously lowers during phase separation, it is equilibrated throughout an inhomogeneous sample at any particular stage of the phase-separation process. The evolving μ_P means a continually changing $f(\rho)$ throughout the phase-separation process, and only asymptotes to the situation in which all three minima lie on a common tangent.

5. Concluding remarks

In this paper, we have expounded a scheme based on earlier suggestions of Cahn [3] whereby permitted kinetic pathways in a system undergoing phase separation can be deduced from the underlying free-energy landscape. The approximate theoretical free-energy landscape is known for any system for which the equilibrium phase behaviour has been calculated; the topology of this landscape can be inferred from the experimental phase diagram in many more cases. Potentially, therefore, a large amount of kinetic information can be obtained by applying this scheme to systems with already-known equilibrium phase behaviour.

While the specific example discussed above was a colloid–polymer mixture, and we expect other applications to come from soft condensed matter, we point out that the scheme is generically applicable. Indeed, Cahn's original motivation was to design phase pathways for the synthesis of glassy metallic alloys. The phase-separation kinetics of water sealed in an isolated, constant-volume container can also be discussed in these terms [8].

Finally, we note that there have been recent attempts at putting the status of concavities in the free-energy landscape (cf. figure 2) on a firm statistical mechanical footing [9].

Acknowledgment

This work was funded by EPSRC Grant GR/K56205.

References

[1] DeHoff R T 1993 *Thermodynamics in Material Science* (New York: McGraw-Hill)
[2] Chaikin P M and Lubensky T C 1995 *Principles of Condensed Matter Physics* (Cambridge: Cambridge University Press) ch 8
[3] Cahn J W 1969 *J. Am. Ceram. Soc.* **52** 118
[4] Anisimov M P, Hopke P K, Rasmussen D H, Shandakov S D and Pinaev V A 1998 *J. Chem. Phys.* **109** 1435
[5] Ghosh O and Miller C A 1987 *J. Phys. Chem.* **91** 4528
[6] Poon W C K, Renth F, Evans R M L, Fairhurst D J, Pusey P N and Cates M E 1999 *Phys. Rev. Lett.* **83** 1239
[7] Lekkerkerker H N W, Poon W C K, Pusey P N, Stroobants A and Warren P B 1992 *Europhys. Lett.* **20** 559
[8] Debenedetti F G 1996 *Metastable Liquids* (Princeton, NJ: Princeton University Press) ch 1
[9] Fisher M E and Zinn S Y 1998 *J. Phys. A: Math. Gen.* **31** L629
Bruce A D 1999 private communication